

## Article

# Study on Precipitation and Dissolution Mechanisms of Graphite in Hot Metal of Blast Furnace

Meng Xie, Hongtao Wang \*, Mingrong Huang, Ping Wang, Yang Song and Zhanxia Di

School of Metallurgical Engineering, Anhui University of Technology, Ma'anshan 243032, China

\* Correspondence: wanghongtao0212@126.com

**Abstract:** Graphite precipitation in the hot metal of a blast furnace (BF) has a significant effect on the low permeability zone of the deadman. In this work, the precipitation mechanisms of graphite in the hot metal of BF were investigated and discussed. Furthermore, the theoretical flame temperature of tuyere raceway, the center temperature of the deadman, and the critical temperature of graphite precipitated from the hot metal, were calculated and the graphitic carbon cycle and graphite enrichment mechanisms in the void of the deadman were analyzed. The results showed that the theoretical flame temperatures of the two BFs used in this study varied from 2100 °C to 2200 °C and the average center temperatures of the deadman in 4350 m<sup>3</sup> and 1280 m<sup>3</sup> BFs were 1329.08 °C and 1386.74, respectively. Moreover, graphite can precipitate from the hot metal and be enriched in the void of the deadman under certain conditions. It was assumed in this work that graphite is precipitated in the form of a 2 mm sphere and the precipitation rate of graphite in hot metal is approximately  $1.01 \times 10^{-8}$  kg/s. With variation in BF conditions, the precipitation–enrichment–dissolution process of graphite occurs continuously in the deadman of the BF.

**Keywords:** low permeability zone; graphite; precipitation and dissolution; hot metal; blast furnace



**Citation:** Xie, M.; Wang, H.; Huang, M.; Wang, P.; Song, Y.; Di, Z. Study on Precipitation and Dissolution Mechanisms of Graphite in Hot Metal of Blast Furnace. *Metals* **2022**, *12*, 1608. <https://doi.org/10.3390/met12101608>

Academic Editors: Emin Bayraktar, Henrik Saxen and Lei Shao

Received: 30 July 2022

Accepted: 22 September 2022

Published: 26 September 2022

**Publisher's Note:** MDPI stays neutral with regard to jurisdictional claims in published maps and institutional affiliations.



**Copyright:** © 2022 by the authors. Licensee MDPI, Basel, Switzerland. This article is an open access article distributed under the terms and conditions of the Creative Commons Attribution (CC BY) license (<https://creativecommons.org/licenses/by/4.0/>).

## 1. Introduction

Hearth activity (representing the smoothness of liquid slag and iron flowing into the hearth and discharging freely from the hearth) is intensely related to the long campaign life of blast furnace (BF) [1–3]. Furthermore, the hearth activity state plays an important role in realizing high efficiency and longevity of BF. According to the erosion mechanisms of the BF layer lining and the low permeability zone in the deadman, analyzed by dissecting dozens of BFs with different volumes throughout the world [4–9], the low permeability zone in the deadman of BF is considered to be the critical factor affecting the hearth activity. During the smelting process of a BF, the main components of burden are iron ore and coke [10,11]. Studies [12,13] have found that the low permeability zone consists of graphite, fine coke particles, slag, and iron. Compared with other regions, the low permeability zone has a smaller porosity, worse air permeability, and lower hearth activity.

As the environment inside the BF is complicated, invisible, and changeable, there is relatively little research on the formation mechanism of the low permeability zone in the deadman and almost no research on graphite enrichment in the low permeability zone. It has been found [14,15] that when the center temperature of the deadman in the hearth of the BF is low, the carbon inside the hot metal can be precipitated in the form of crystal graphite, which together with residual ash, coke fines, and unburned pulverized coal in the hearth may block the void of the deadman. The relationship between the heat transfer coefficient and the BF bottom temperature, as well as the low permeability zone of the hearth, had been discussed by Sawa et al. [16]. Many studies have shown that temperature is one of the important factors influencing the precipitation of graphite from hot metal [17–19]. In the actual operation of a BF, the central temperature of the deadman (DMT) is difficult to be identified, while the theoretical flame temperature (*TTT*) of the raceway related to the DMT

is easy to calculate. Consequently, to provide theoretical support for further investigation into the formation mechanism of the low permeability zone in the deadman, the DMT was calculated through the theoretical flame temperature and the mechanism of carbon precipitation in the hot metal was studied. Simultaneously, the graphite cycle and the mechanisms of graphite enrichment in the void of the deadman were further analyzed. This paper could provide a theoretical foundation for the formation of the low permeability zone in the deadman and the longevity of the BF.

## 2. Center Temperature of the Deadman in the BF Hearth

The BF is considered to be one of the most complex metallurgical reactors, and the BF smelting process cannot be observed directly. Via long-term research and exploration, it has been determined that the hearth activity state is important for estimating the actual running operation of the BF. Furthermore, the DMT is a significant parameter for identifying the hearth activity, which mainly depends on the *TTT* of the raceway, the bosh gas volume, the fuel rate, and the CO utilization efficiency at the furnace center.

### 2.1. Theoretical Flame Temperature of the BF

The *TTT* of the tuyere raceway is mainly used to evaluate the thermal state inside the BF, which can be applied to direct the BF operation and ensure the stability and smoothness of BF smelting. Currently, the *TTT* is commonly calculated by an empirical equation (Equation (1)) [20,21].

$$TTT = 0.74T_f - 1.6M - 7.6M_{O_j} + 40F_O + 1565.59 \quad (1)$$

where *TTT* is the theoretical flame temperature (°C), *T<sub>f</sub>* is the blast temperature (°C), *M* is the coal ratio (kg/t), *M<sub>O<sub>j</sub></sub>* is the blast humidity (g/m<sup>3</sup>), and *F<sub>O</sub>* is the oxygen enrichment (%).

The *TTT* of the BF under a normal running state is reported between 2000 °C and 2200 °C [22]. Tables 1 and 2 present the operation data of 4350 m<sup>3</sup> and 1280 m<sup>3</sup> BFs in steelworks, respectively. The *TTT*s of the two BFs were calculated according to Equation (1), as shown in Tables 1 and 2. The *TTT* of the BF with a volume of 4350 m<sup>3</sup> fluctuates between 2109.0 °C and 2191.6 °C, with an average value of approximately 2142.8 °C. In comparison to the 4350 m<sup>3</sup> BF, the *TTT* variation range of the 1280 m<sup>3</sup> BF is larger, from 2044.2 °C to 2198.1 °C. The average *TTT* of the 1280 m<sup>3</sup> BF is approximately 2133.9 °C.

**Table 1.** Operation data of the 4350 m<sup>3</sup> BF in steelworks.

Item	<i>M</i> /(kg/t)	<i>T<sub>f</sub></i> /°C	<i>M<sub>O<sub>j</sub></sub></i> /(g/m <sup>3</sup> )	<i>F<sub>O</sub></i> /%	<i>TTT</i> /°C
1	141.0	1228.0	28.7	1.96	2109.0
2	153.0	1233.0	29.4	2.57	2112.6
3	146.0	1210.0	26.8	2.73	2132.9
4	146.7	1223.0	28.3	2.43	2118.0
5	145.0	1213.0	21.5	2.67	2174.6
6	149.0	1228.0	20.2	2.73	2191.6
7	158.0	1210.0	23.2	2.62	2136.7
8	150.6	1217.0	21.7	2.67	2142.5
Average	148.6	1220.2	24.98	2.54	2142.8

**Table 2.** Operation data of the 1280 m<sup>3</sup> BF in steelworks.

Item	M/(kg/t)	T <sub>f</sub> /°C	M <sub>Oj</sub> /(g/m <sup>3</sup> )	F <sub>O</sub> /%	TCT/°C
1	105.94	1158.74	21.82	0.95	2125.8
2	80.45	1111.41	29.26	1.22	2085.8
3	65.21	1082.65	34.76	1.15	2044.2
4	76.27	1135.52	23.81	1.31	2155.3
5	102.13	1177.23	19.95	1.22	2170.5
6	102.17	1168.69	23.90	1.44	2142.9
7	101.71	1207.52	19.72	1.29	2198.1
8	119.32	1170.90	18.49	1.19	2148.2
Average	94.15	1151.58	23.96	1.22	2133.9

## 2.2. Center Temperature of the Deadman in the Hearth

The DMT in the hearth is a significant factor for estimating the hearth activity. A higher DMT indicates a better hearth activity. Raipala et al. [20,23] proposed a method for calculating the DMT, which is shown in Equation (2).

$$\text{DMT} = \frac{0.165 \times TTT \times V_{\text{bosh}}}{D^3} + 2.445(FR - 483) + 2.91(\Delta t - 107) - 11.2(\eta_{\text{CO.C}} - 27.2) + 28.09(D_{\text{pcoke}} - 25.8) + 326 \quad (2)$$

where DMT is the center temperature of the deadman (°C);  $V_{\text{bosh}}$  is the volume of the bosh gas inside the BF (m<sup>3</sup>/min);  $\eta_{\text{CO.C}}$  is the utilization efficiency of CO at the furnace center measured by a shaft probe (%);  $D_{\text{pcoke}}$  is the size of coke in the core of the deadman (mm);  $D$  is the hearth diameter (m);  $FR$  is the fuel ratio (kg/t); and  $\Delta t$  is the slag flow index, defined as the difference between the tapping temperature of the BF and the flow temperature of the slag in the BF (°C) [24].

As tuyere probing was carried out, the coke quality parameters and the operation parameters of two BFs with different volumes in steelworks were analyzed and listed in Tables 3 and 4. The DMT is 1380~1450 °C with the normal production of the BF [25]. On the basis of Equation (2), the DMT of the 4350 m<sup>3</sup> BF is 1270.72~1412.48 °C and the average value is approximately 1329.08 °C. In addition, the DMT of the 1280 m<sup>3</sup> BF is between 1278.75 °C and 1494.01 °C and the average core temperature is about 1386.74 °C. With increasing the amount of hot metal flowing through the deadman, the DMT rises, indicating that the void of the deadman is large and gas permeability and liquid permeability are high. As a result, the hearth activity is favorable. However, when the DMT is lower than 1380 °C, even lower than the melting temperature of slag, the slag viscosity increases and the slag fluidity decreases. As a consequence, the hearth activity worsens and BF stability deteriorates.

**Table 3.** Coke quality parameters and operation parameters of the 4350 m<sup>3</sup> BF in steelworks.

Item	TTT/°C	V <sub>bosh</sub> /(m <sup>3</sup> /min)	η <sub>CO.C</sub> /%	D <sub>pcoke</sub> /mm	D/m	FR/(kg/t)	Δt/°C	DMT/°C
1	2109.0	10,802	51.8	28.5	14	495.3	67.9	1412.48
2	2112.6	10,222	51.4	27.6	14	486.5	69.2	1302.60
3	2132.9	10,287	51.9	25.5	14	521.3	49.1	1285.44
4	2118.0	11,109	51.7	26.3	14	470.9	54.3	1346.43
5	2174.6	10,459	51.9	27.5	14	501.8	43.1	1324.77
6	2191.6	10,058	52.0	28.1	14	506.4	48.5	1325.30
7	2136.7	9635	51.5	26.1	14	503.8	79.4	1270.72
8	2167.1	9717	51.8	29.7	14	518.5	56.1	1364.93
Average	2142.8	9911.12	51.75	27.4	14	500.6	58.45	1329.08

**Table 4.** Coke quality parameters and operation parameters of the 1280 m<sup>3</sup> BF in steelworks.

Item	TTT/°C	V <sub>bosh</sub> /(m <sup>3</sup> /min)	η <sub>CO,C</sub> /%	D <sub>pcoke</sub> /mm	D/m	FR/(kg/t)	Δt/°C	DMT/°C
1	2125.8	3192.92	45.6	25.5	9.5	508	48.7	1309.21
2	2085.8	2987.58	46.3	28.6	9.5	541	59.6	1393.85
3	2044.2	2957.3	46.2	27.9	9.5	507	67.3	1278.75
4	2155.6	2690.41	42.5	27.1	9.5	561	41.1	1306.03
5	2170.5	3303.25	44.27	26.5	9.5	510	59.3	1461.48
6	2142.9	3257.12	43.9	26.4	9.5	512	68.1	1456.75
7	2198.1	3251.976	44.1	27.2	9.5	502	36.8	1393.87
8	2148.2	3283.03	44.07	27.9	9.5	506	67.3	1494.01
Average	2133.9	3115.375	44.62	27.1	9.5	518.3	56.025	1386.74

### 3. Results and Discussion

#### 3.1. Precipitation Temperature of Graphite in Hot Metal

At a certain temperature, carbon deposition reaction can occur when the carbon dissolved in hot metal is saturated. The reaction is as follows [26].

$$[C] = C \quad \Delta G^{\theta} = 22590 - 42.26T \quad (3)$$

In the reaction, pure graphite is the reference state for [C] and the henry activity of the dissolved carbon is given by  $f_C$  [%C].

The Gibbs free energy variation of the above-mentioned reaction can be generally expressed as follows:

$$\Delta G = 22,590 - 42.26T + RT \ln \frac{1}{f_C [\%C]} \quad (4)$$

where  $f_C$  is the activity coefficient of carbon in hot metal and [%C] is the carbon concentration in hot metal. The logarithm of the activity coefficient of carbon at 1600 °C can be determined by Equation (5) [26].

$$\lg f_{C1600^{\circ}C} = e_C^C [\%C] + e_C^{Si} [\%Si] + e_C^{Mn} [\%Mn] + e_C^P [\%P] + e_C^S [\%S] + e_C^{Cr} [\%Cr] \quad (5)$$

where  $e^i_j$  represents the interaction coefficient between elements  $i$  and  $j$  in hot metal and [%i] is the content of element  $i$  in hot metal. The interaction coefficient between other elements and carbon at 1600 °C is listed in Table 5, while Tables 6 and 7 present the compositions of the hot metal derived from the production data of the above two BFs, respectively. Since it is difficult to actually measure the composition of the hot metal in the deadman, the composition of the metal inside the deadman is assumed to be the same as that in the taphole.

**Table 5.** Interaction coefficient between other elements and carbon in hot metal at 1600 °C, data from [26].

Element	C	Si	Mn	P	S	Cr
Interaction coefficient ( $e^i_C$ )	0.14	0.08	−0.012	0.051	0.046	−0.12

**Table 6.** Composition of hot metal derived from the 4350 m<sup>3</sup> BF.

Hot Metal Composition	C	Si	Mn	P	S	Cr
Content/%	4.80	0.35	0.35	0.15	0.014	0.06

**Table 7.** Composition of hot metal derived from the 1280 m<sup>3</sup> BF.

Hot Metal Composition	C	Si	Mn	P	S	Cr
Content/%	4.731	0.423	0.208	0.122	0.024	0.005

Furthermore, the activity coefficient of carbon at different temperatures can be calculated by that at 1600 °C, as shown in Equation (6).

$$\lg f_C = \left( \frac{2538}{T} - 0.355 \right) \lg f_{C1600^\circ\text{C}} \quad (6)$$

The critical temperature of graphite precipitation in hot metal is calculated according to Equations (3)–(6), together with the data in Tables 5 and 6, and is found to be about 1382 °C for the 4350 m<sup>3</sup> BF. From the above results, the DMT for this BF is between 1270.72 °C and 1412.48 °C. As a result, when the temperature of the hot metal is lower than 1382 °C, the graphite can be precipitated in the crystalline form and enriched in the void of the deadman. As the temperature is higher than 1382 °C, the precipitated graphite can be dissolved again in the hot metal. Therefore, the precipitation–enrichment–dissolution process of graphite is continuous in the hearth with variation in BF conditions.

The critical temperature of graphite precipitation in hot metal in the 1280 m<sup>3</sup> BF can be calculated by Equations (3)–(6) and the data in Tables 5 and 7, which is approximately 1359 °C. Consequently, when the temperature of the hot metal is lower than 1359 °C, the carbon deposition reaction can proceed in the hot metal. The DMT of this small BF is about 1278.75–1494.01 °C. As a result, when the temperature of the hot metal is below 1359 °C, the graphite can be precipitated in a crystalline form and be enriched in the void of the deadman. However, when the temperature of the hot metal is greater than 1359 °C, the precipitated carbon dissolves in the hot metal. With a variation in the BF conditions, the graphite constantly undergoes the precipitation-enrichment-dissolution process.

Therefore, what happens to the graphite in the hot metal can vary in BFs with different volumes since the DMT fluctuates due to the change in BF conditions. The critical temperature of graphite precipitation may also differ when the composition of the hot metal is changed, especially the content of carbon and sulfur in the hot metal.

### 3.2. Precipitation Rate of Graphite

The solubility of graphite in hot metal differs with temperature. At lower temperature of hot metal, graphite has lower solubility. When the temperature of the hot metal is lower than the precipitation critical temperature of graphite, the carbon in the hot metal will precipitate in the crystalline form, generating a boundary layer of graphite with a certain concentration in the void of the deadman, which contributes to the generation of a low liquid permeability zone. The precipitation rate of graphite can be presented as Equation (7) [26].

$$v = \frac{dM_s}{dt} = \beta A \rho [w(C) - w(C)_s] \quad (7)$$

where  $M_s$  is the mass of precipitated carbon (kg),  $\beta$  is the mass transfer coefficient of melt component  $w(C)$  (m/s),  $A$  is the interface area between solid and melt (m<sup>2</sup>),  $\rho$  is the density of the graphite (kg/m<sup>3</sup>),  $w(C)$  is the carbon concentration in hot metal, and  $w(C)_s$  is the saturated concentration of carbon at a certain temperature in hot metal.

The mass transfer coefficient of carbon in hot metal ( $\beta$ ) is approximately  $2.41 \times 10^{-4}$  m/s, and the density of graphite ( $\rho$ ) is about 2460 kg/m<sup>3</sup> [26]. The graphite in the deadman between the taphole and the bottom surface of the BF is in the form of tiny particles, so it is assumed that the graphite is precipitated in the form of spheres and that the final radius ( $r$ ) of the precipitated graphite is about 0.001 m [16]. So, the largest value of  $A$  is considered to be the surface area of the largest sphere ( $4\pi r^2$ ) [16]. When the average DMT is 1329.08 °C, the concentration of carbon in hot metal ( $w(C)$ ) is approximately 4.72%. According to the above, the precipitation temperature of the graphite in the hot metal of the large BF is 1382 °C and the concentration of carbon in the hot metal ( $w(C)_s$ ) is approximately 4.85%.

The maximum precipitation rate of graphite in hot metal is calculated to be approximately  $1.01 \times 10^{-8}$  kg/s, as follows:

$$\begin{aligned} v &= \beta A \rho [w(C) - w(C)_s] \\ &= 2.41 \times 10^{-4} \times 4 \times \pi \times (1 \times 10^{-3})^2 \times 2460 \times (4.85\% - 4.72\%) \\ &= 1.01 \times 10^{-8} \text{ kg/s} \end{aligned} \quad (8)$$

The low permeability zone in the deadman of the BF may become large with increasing the precipitation amount of graphite according to the relationship between the precipitation of graphite and the permeability of the deadman. During the actual production of the BF, the BF condition can be regulated by adjusting the process parameters according to the graphite precipitation time. Thus, the precipitation time ( $t$ ) required for the maximum contact area during the precipitation process of graphite is calculated by Equation (9). The precipitation time is approximately 17.7 min.

$$\begin{aligned} t &= \frac{V \times \rho}{v} = \frac{\frac{4}{3} \pi r^3 \times \rho}{\beta 4 \pi r^2 \rho [w(C) - w(C)_s]} = \frac{r}{3 \beta [w(C) - w(C)_s]} \\ &= \frac{1 \times 10^{-3}}{3 \times 2.41 \times 10^{-4} \times (4.85\% - 4.72\%)} = 1064 \text{ s} = 17.7 \text{ min} \end{aligned} \quad (9)$$

### 3.3. Circulation and Enrichment of Graphite in the Deadman

The precipitation and dissolution mechanisms of graphite in the hot metal of a BF hearth are demonstrated in Figure 1. With the variation in BF conditions, graphite in the hot metal undergoes a continuous cycle of precipitation, enrichment, and dissolution. When the hearth is inactive, the hot metal mainly circulates. Only a small amount of the hot metal flows through the bottom and the interior of the deadman, causing an increase in the temperature of the hearth sidewall and a decrease in the temperature inside the deadman as well as of the hearth bottom. According to the previous theoretical calculation, the precipitation temperature of graphite is just in the temperature range of the DMT. Therefore, when the temperature of the hot metal is lower than the precipitation temperature of graphite, the graphite can be continuously precipitated in the form of crystals and enriched in the void of the deadman. With passage of time, the amount of enriched graphite increases. As a result, the void of the deadman decreases, which can decrease the heat in hot metal as well as the flow rate of the hot metal through the deadman. Therefore, the temperature inside the deadman gradually decreases. In this case, the graphite can precipitate more easily in the void of the deadman, leading to the deterioration of the deadman and the formation of a low liquid permeability region.

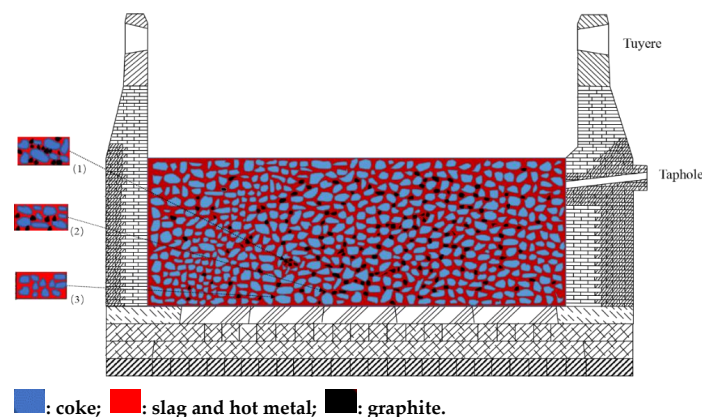


**Figure 1.** Diagram of precipitation and disappearance of graphite in the BF hot metal. (1) : Graphite is enriched in the deadman. (2) : Graphite is precipitated in hot metal. (3) : Graphite is dissolved in hot metal.

When the hearth is active, most of the hot metal flows from the bottom of the deadman to the taphole, which can cause the temperature to increase at the bottom of the deadman and decrease at the hearth sidewall. The temperature of hot metal is higher than the precipitation temperature of graphite, and when the temperature of hot metal rises, the corresponding saturated solubility of carbon increases. As a result, graphite dissolves in the hot metal. According to the research of Sawa [16], most of the graphite precipitation in the inactive period is carried out by the slag at the initial stage when the hearth changes from inactive to active. Therefore, the graphite layer enriched in the void of the deadman will be partly dissolved in the hot metal with a high temperature and the graphite is gradually taken away from the void of the deadman by the hot metal.

BF ironmaking is complex and variable. The variations inside a BF can only be deduced from relevant data and are impossible to evaluate directly. However, what has been confirmed is that the DMT fluctuates constantly within a certain range and the graphite undergoes a continuous precipitation-enrichment-dissolution process in the void of the deadman.

#### 4. Conclusions

In this paper, the precipitation process of graphite in hot metal was discussed and the relevant parameters of two BFs with different volumes were calculated. The following conclusions were drawn:

1. For the 4350 m<sup>3</sup> BF, the center temperature of the deadman is 1270.72~1412.48 °C and the critical temperature of the graphite precipitation in hot metal is about 1382 °C. The maximum rate of precipitation to form a 2 mm graphite sphere is  $1.01 \times 10^{-8}$  kg/s, and the time is approximately 17.7 min.
2. As the furnace temperature varies, the graphite undergoes precipitation, enrichment, and dissolution in the void of the deadman. When the graphite is enriched, a low-permeability zone is formed in the deadman.

**Author Contributions:** Conceptualization, P.W.; methodology, Z.D. and H.W.; investigation, M.X. and Y.S.; writing—original draft preparation, M.X. and Y.S.; writing—review and editing, H.W. and M.H.; funding acquisition, Z.D. and H.W. All authors have read and agreed to the published version of the manuscript.

**Funding:** This research was supported by the National Natural Science Foundation of China (52004001) and the Projects of University Natural Science Research Project in Anhui Province (KJ2018A0045).

**Institutional Review Board Statement:** Not applicable.

**Informed Consent Statement:** Not applicable.

**Data Availability Statement:** Not applicable.

**Conflicts of Interest:** The authors declare no conflict of interest.

#### References

1. Chen, H.; Wu, S.L.; Yu, X.B. New index of evaluating activity of blast furnace hearth. *Iron Steel* **2007**, *42*, 12–16.
2. Zhang, J.L.; Jiao, K.X.; Liu, Z.J.; Yang, T.J. Comprehensive regulation technology for hearth protective layer of blast furnace longevity. *Iron Steel* **2017**, *12*, 1–7.
3. Zhang, W.Z. Analysis and discussion on the activity of blast furnace hearth. *Shandong Metall.* **2022**, *1*, 21–22+26.
4. Jiao, K.X.; Zhang, J.L.; Liu, Z.J.; Yang, T.J. Analysis of key issues on longevity of blast furnace hearth. *Iron Steel* **2020**, *8*, 193–198.
5. Zhang, J.L.; Wang, Z.Y.; Jiao, K.X.; Wang, C.; Zhao, Y.A. Slag erosion resistance and hanging mechanism for the refractory in blast furnace hearth. *Iron Steel* **2015**, *11*, 27–31.
6. Zhao, Q.Q.; Chen, T.; Zhao, G.L.; Wang, L.X. Design and practice of blast furnace longevity hearth. *Tianjin Metall.* **2020**, *3*, 5–7+26.
7. Wang, G.; Li, A.F.; Liu, F.J.; Chen, G.Z.; Xu, J.; Liu, Z.B. Development and application of intelligent management system for blast furnace hearth longevity. *China Metall.* **2016**, *4*, 43–46.
8. Wang, C.; Zhang, J.L.; Chen, W.; Li, X.L.; Jiao, K.X.; Pang, Z.P.; Wang, Z.Y.; Wang, T.S.; Liu, Z.J. Comparative analysis on the corrosion resistance to molten iron of four kinds of carbon bricks used in blast furnace hearth. *Metals* **2022**, *12*, 871. [[CrossRef](#)]

9. Ni, A.; Li, C.; Zhang, W.; Xiao, Z.; Liu, D.; Xue, Z. Investigation of the hearth erosion of WISCO No.1 blast furnace based on the numerical analysis of iron flow and heat transfer in the hearth. *Metals* **2022**, *12*, 843. [CrossRef]
10. He, K.; Wang, L.; Li, X.Y. Review of the energy consumption and production structure of China's steel industry: Current situation and future development. *Metals* **2020**, *10*, 302. [CrossRef]
11. Tang, H.Q.; Yun, Z.W.; Fu, X.F.; Du, S. Modeling and experimental study of ore-carbon briquette reduction under CO–CO<sub>2</sub> atmosphere. *Metals* **2018**, *4*, 205. [CrossRef]
12. Wang, X.L.; Jiao, K.X.; Qi, C.L.; Xiang, Z.Y. Formation mechanism and influencing factors of carbon brick protection layer in BF hearth. *Ironmaking* **2017**, *5*, 8–14.
13. Wen, X.; Zou, Z.P.; Jiang, H.; Wang, W.; Zheng, S.B.; Yu, Z.D. Composition analysis and thermal conductivity measurement of iron skull in blast furnace hearth. *J. Iron Steel Res.* **2019**, *9*, 779–786.
14. Zhang, L.L. Control of Side Wall Erosion of Hearth from the “Core”. 2014. Available online: <http://www.csteelnews.com/ztbd/cmn/> (accessed on 29 July 2022).
15. Zhang, W.; Hua, F.B.; Dai, J.; Xue, Z.L.; Ma, G.J.; Li, C.Z. Isothermal kinetic mechanism of coke dissolving in hot metal. *Metals* **2019**, *9*, 470. [CrossRef]
16. Sawa, Y.; Takeda, K.; Taguchi, S.; Matsumoto, T.; Toshiyuki, W.; Kamano, H. Influence of low permeability zone in blast furnace hearth on temperature distribution in furnace bottom and on iron and slag tapping indices. *Tetsu-to-Hagane* **2009**, *7*, 1171–1178.
17. Jiao, K.X.; Zhang, J.L.; Zuo, H.B.; Zhao, Y.A. Composition and formation mechanism of viscous layers in blast furnace hearth. *J. Northeast Univ. (Nat. Sci.)* **2014**, *35*, 987–991.
18. Xie, R.J. Analysis of influencing factors on hot metal viscosity of blast furnace in MInguang Company of Quanzhou. *Tianjin Metall.* **2020**, *6*, 14–18+26.
19. Xu, K. Study on Technology of High-Value Utilization of Carbon Precipitation at Ironmaking-Steelmaking Interface Due to Temperature Drop. Master's Thesis, Northeastern University, Shenyang, China, 2019.
20. Raipala, K. *On Hearth Phenomena and Hot Metal Carbon Content in Blast Furnace*; Helsinki University of Technology: Helsinki, Finland, 2003.
21. Wang, Y.S.; Zhu, W.C. The discuss of theory flame temperature experience formula at the Shougang BFs. In Proceedings of the 2003 CSM Steel Congress, Beijing, China, 28–30 October 2003.
22. Zhou, H.; Xu, K.; Yao, S.; Kou, M.Y.; Wu, S.L. Numerical simulation of injection of COREX decarbonized top gas to blast furnace. *Iron Steel* **2021**, *2*, 57–62.
23. Raipala, K. Deadman and hearth phenomena in the blast furnace. *Scand. J. Metall.* **2000**, *29*, 39–46. [CrossRef]
24. Dai, B.; Liang, K.; Wang, X.J.; Li, X.; Guo, Y.W. Development and practice of quantitative calculation models of blast furnace hearth activity. *China Metall.* **2015**, *25*, 45–49.
25. Dai, B.; Liang, K.; Wang, X.J.; Hui, G.D.; Dong, H.; Sun, H.J. Fundamental research on hearth activity of blast furnace. In Proceedings of the 10th CSM Steel Congress and the 6th Baosteel Biennial Academic Conference, Shanghai, China, 21–23 October 2015.
26. Jiao, K.X.; Zhang, J.L.; Liu, Z.J.; Liu, F.; Liang, L.S. Formation mechanism of the graphite-rich protective layer in blast furnace hearths. *Int. J. Miner. Metall. Mater.* **2016**, *1*, 16–24. [CrossRef]